

Chemically Induced Dimerization of Human Nonpancreatic Secretory Phospholipase A2 by Bis-indole Derivatives

Lu Zhou,[†] Chao Fang,[†] Ping Wei,[†] Shiyong Liu,^{†,‡} Ying Liu,^{*,†} and Luhua Lai^{*,†,‡}

Beijing National Laboratory for Molecular Sciences, State Key Laboratory for Structural Chemistry of Unstable and Stable Species, College of Chemistry and Molecular Engineering, Peking University, Beijing 100871, China, and Center for Theoretical Biology, Peking University, Beijing 100871, China

Received August 30, 2007

A series of novel bis-indole compounds, 1, ω -bis(((3-acetamino-5-methoxy-2-methylindole)-2-methylene)phenoxy)alkane, have been designed and synthesized on the basis of the enzyme structure of human nonpancreatic secretory phospholipase A2 (hnps PLA2). Their inhibition activities against hnps PLA2 were improved compared to that of the monofunctional protocompound. These bivalent ligands not only inhibited hnps PLA2 but also drove the dimerization of hnps PLA2. Their dimerization ability correlated with the linker length and position. Further study on the potent compound **5** (1,5-bis(((3-acetamino-5-methoxy-2-methylindole)-2-methylene)phenoxy)pentane, IC₅₀ = 24 nM) revealed that cooperative binding interactions between the two enzyme molecules also contributed to the stability of the ternary complex. The combination of bivalent ligands and hnps PLA2 can be used as a novel chemically induced dimerization (CID) system for designing regulatory inhibitors.

Introduction

Dimerization and oligomerization are general biological control mechanisms that contribute to the activation of intra- and extracellular proteins, including cell membrane receptors and vesicle fusion proteins.^{1,2} Chemically induced dimerization (CID^a) systems have been used to manipulate cellular regulatory pathways from signal transduction to transcription by inducing dimerization of key proteins. The concept of CID systems was first exploited by Schreiber and Crabtree in their pioneering design of FK1012 (**27**, a dimeric form of tacrolimus (FK506) (**28**)).² This approach has yielded several novel CID systems^{3–7} and has been applied to important biological systems such as the RNA–protein complex⁸ and heterodimeric complex.⁹ In fact, inhibitors capable of inducing HIV-1 reverse transcriptase dimerization exhibited increased binding strength.¹⁰ Even though these examples demonstrate the general feasibility of modulating protein–protein interactions with small organic molecules, the application of this principle to drug discovery research has encountered many obstacles. Berg¹¹ pointed out three main problems: (1) the identification of lead compounds is difficult; (2) the protein–protein interface is much larger than the potential binding area of a low molecular weight compound; (3) protein–protein interfaces are often flat and may therefore lack binding sites for small molecules. Because of these difficulties, it is a challenge to find small molecules that can modulate protein–protein interactions and to characterize the cooperative nature of these interactions. Thus, although CID is

useful as a regulatory tool in biological systems, the number of known CID systems is limited.

Phospholipase A2 (PLA2, EC 3.1.1.4) hydrolyzes the acyl-ester bond at the sn-2 position of phosphoglycerides and liberates free fatty acids, predominantly arachidonic acid, and lysophospholipids. Overexpression of PLA2 is believed to play an important role in the inflammatory process.^{12,13} As a membrane-bound enzyme,¹⁴ PLA2 has an *i*-face that has been proposed to make contact with the substrate interface, leading to the interfacial catalytic turnover.¹⁵ The *i*-face of PLA2 is a relatively flat surface of 1600 Å², which binds tightly to the phospholipid bilayer ($K_d < 10^{-13}$ M). There are some polarizable and hydrophobic residues on the flat surface, through which PLA2 binds to the anionic bilayer. The *i*-faces have been found to interact with each other under certain circumstances, and two crystal structures containing PLA2 dimers have been reported.^{16–18} The catalytic residues were buried by the dimer interface and were inaccessible from the bulk solvent. The free-energy minimization process might exclude the hydrophobic molecular surface from the aqueous solution, but PLA2s were all detected as monomers in aqueous solution. It seemed that the interaction between two PLA2s was weak and not exclusive.

As described above, the application of CID systems to drug research remains challenging. Fortunately, all of the noted difficulties were avoided in the present study. The identification of lead compounds is easy for hnps PLA2. Many potent inhibitors against hnps PLA2 were reported. The secretory PLA2 is an interfacial enzyme with its active pocket near the substrate binding *i*-face. The small molecule could act as an inducer to pull two protein molecules together and let them interact with each other. Thus, the last two problems were solved at the same time. PLA2 simultaneously provides the binding site for small molecules and the protein–protein interaction surface, providing good conditions for CID studies. Since the buried *i*-face plays an important role in binding to the phospholipid surface, we

* To whom correspondence should be addressed. For Y.L.: phone, 86-10-62751490; fax, 86-10-62751725; e-mail, liuying@pku.edu.cn. For L.L.: phone, 86-10-62757486; fax, 86-10-62751725; e-mail, lhlai@pku.edu.cn.

[†] College of Chemistry and Molecular Engineering.

[‡] Center for Theoretical Biology.

^a Abbreviations: hnps PLA2, human nonpancreatic secretory phospholipase A2; CID, chemically induced dimerization; IC₅₀, inhibition constant; K_a, association constant.

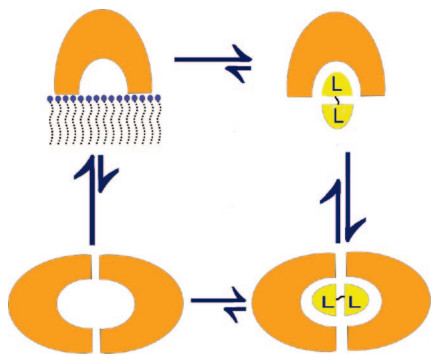


Figure 1. Strategy of bivalent inhibitor design. The bivalent inhibitor can induce PLA2 molecules to form a dimer at the *i*-face to prevent their binding to the lipid surface.

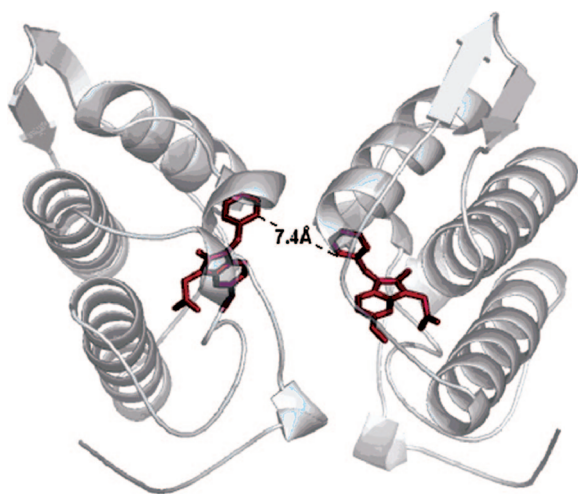


Figure 2. Dimer model of hnpS PLA2. The protein molecules are shown as ribbons, and the small molecules are shown as stick models. The structure is similar to that of the pancreatic IB PLA2 dimer induced by MJ33 (1-hexadecyl-3-(trifluoroethyl)-*sn*-glycero-2-phosphomethanol).¹⁸ The small molecule is half of the dimerizer, and the distance between the two phenyl rings' ortho position is 7.4 Å. The figure was prepared using PyMOL.²³

postulated that compounds that can induce dimerization of PLA2, thus burying the *i*-face, may increase the binding affinity of the monomers and regulate enzyme activity (Figure 1).

We have developed a novel CID system using phospholipase A2 as the target protein and a bivalent inhibitor as the chemical linker. The design of the bivalent ligand was based on the protein dimer model, where two molecules of the human nonpancreatic secretory PLA2 (hnpS PLA2) were each bound to an indole derivative **1** (5-methoxy-2-methyl-1*H*-1-benzyl-indole-3-acetamide) (PDB code 1DB4)¹⁹ reported to be a potent hnpS PLA2 inhibitor.²⁰ Bis-indole derivatives **3–11** were synthesized to contain two compound **1** molecules linked with an alkyl ether chain of varying length. These compounds could drive the dimerization of hnpS PLA2 as confirmed by analytical ultracentrifugation and were found to be potent hnpS PLA2 inhibitors using continuous fluorescence assay.²¹

Results

Molecular Modeling Studies. To design bivalent ligands, we first built a dimer model for hnpS PLA2 using the hnpS PLA2 monomer (PDB code 1DB4) and the FTDOCK program²² (Figure 2). In the model, the *i*-faces were buried at the interface of the dimer and the two substrate binding pockets formed a

capsule. We docked the known inhibitor **1** ($IC_{50} = 0.84 \mu M^{20}$) into the substrate binding pocket of each monomer enzyme. The hydrophobic group of each inhibitor molecule is close to the interface and exposed to the other pocket. The minimal length between the two phenyl rings of the inhibitor is approximately 7 Å, about seven C–C bond lengths. Because of their distance and conformation, the two phenyl rings can be linked together to form a homobifunctional inhibitor. An alkyl chain would be a favorable linker because it can occupy the hydrophobic capsule inside the PLA2 dimer. Since the exact chemical composition of an optimal spacer is difficult to predict, we synthesized bivalent ligands with alkyl spacers ranging from 3 to 9 at various substitution positions.

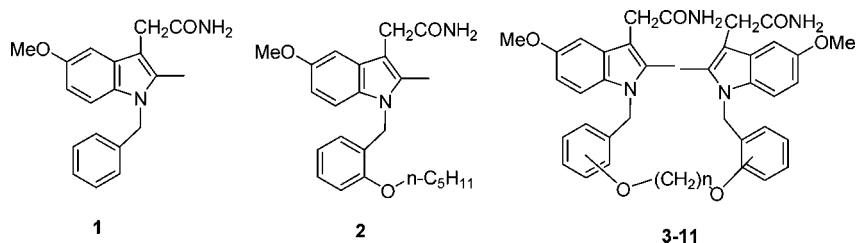
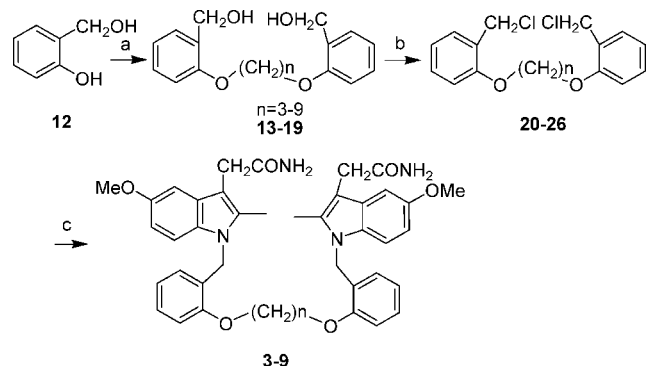
Synthesis of Bivalent Ligands. In order to modulate the spacer length by one-atom increments with homogeneous chemical compositions, we synthesized a series of compounds (shown in Schemes 1 and 2). The compounds **3–11** were synthesized in three steps: (a) Compounds **13–19** were prepared by nucleophilic substitute reaction of molecule **12** and 1, ω -dibromoalkane (the mole ratio was 2:1). (b) The hydroxymethyl of compounds **13–19** was converted to chloromethyl to yield compounds **20–26**. (c) **3–11** were obtained by the reaction of compounds **20–26** with 5-methoxy-2-methyl-1*H*-indole-3-acetamide.²⁴ **10** and **11** were started from 3-hydroxyphenylmethanol and 4-hydroxyphenylmethanol, respectively, and the linker was 1,5-dibromopentane. The structures of compounds **3–11** were confirmed by ¹H NMR, MS, and elemental analysis. In order to check for the influence of the linker on the inhibition activity, a monovalent compound **2** with a linker was synthesized by steps similar to those for compounds **3–11** but the dibromoalkane was changed to 1-bromopentane.

Dimer Induction Study. Sedimentation experiments can study the aggregation state of proteins in native solution, and no dilution effect exists compared to gel filtration, which may cause inhibitor deposition. Peter Schuck has developed a method for the analysis of protein self-association by sedimentation velocity experiments.²⁷ Sedimentation velocity provides hydrodynamic information about molecular size distribution and conformational changes.^{25,26} We used sedimentation velocity experiments to determine the dimerization of hnpS PLA2 in the presence of inhibitors.

All the inhibitors were tested against hnpS PLA2 for their ability to induce dimers (Figure 3). The relative peak areas are approximately equal to the proportions of monomer and dimer based on their absorbance. From the result, we can see that **3–6** could induce the dimerization of hnpS PLA2 in the order **5** > **3** ~ **6** > **4**. **7** showed only a weak ability to induce dimers, while the other compounds showed no inducement. Although **10** (meta-substituting) and **11** (para-substituting) have the same alkyl chain length as **5**, they could not induce the dimerization of hnpS PLA2 (data not shown). This means that the dimerization ability of the compounds is influenced by both the length of the linker and the position of the substituent. Compound **5** has an optimal alkyl chain length and position that fits the capsule of the dimer well. Figure 2 shows that the distance of the two phenyl rings of the monofunctional inhibitors is about 7.4 Å, which correlates well with the linker length of compound **5**.

Compound **5** was further studied for its mechanism of dimer induction. Carlson and co-workers gave a method to estimate K_{eq} and K_c values when the dimerizer possessed conformational equilibria.²⁸ The effects of ligand conformational equilibria (K_{eq}) and cooperative receptor interactions (K_c) modulate the values

Scheme 1. Chemical Structures of Bivalent Inhibitors and the Two Lead Compounds

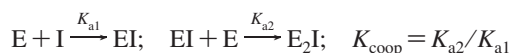
Scheme 2. Synthetic Route of Compounds 3–9^a

^a (a) $\text{Br}(\text{CH}_2)_n\text{Br}$ ($n = 3-9$), K_2CO_3 , CH_3CN ; (b) PPh_3 , CCl_4 ; (c) 5-methoxy-2-methyl-1*H*-indole-3-acetamide, NaH , DMF .

of K_{a1} and K_{a2} , respectively.²⁸ A concentration-dependent sedimentation experiment was carried out (Figure 4a) to evaluate the cooperative interactions at the PLA2 interface. The fraction of protein in the ternary complex is shown as a function of the ratio of compound **5** to PLA2. When the ratio of **5**/PLA2 was increased from 0.0 to 0.5, the dimer percentage increased from zero to a peak value of around 0.75. When the inhibitor concentration was further increased, the dimer percentage started to decrease, showing that the binding model of **5** and hnp PLA2 changed from 1:2 to 1:1. Because of the limited solubility of compound **5**, the maximal concentration of **5** was twice that of PLA2. From the data available, the K_c value was small and the cooperative interaction was not very strong. A competition experiment with the monovalent ligand was carried out to assess the possible impact of the hydrophobic collapse of the bis-indole compound in water on dimerization (Figure 4b). The fraction of ternary complex decreased slowly, indicating that K_{coop}/K_c is relatively small, which implied that the effect of ligand conformational equilibria played a minor role in the dimerization process. Because compound **5** contains a linker of five C–C bonds, it may be too short for the molecule to fold up. We also checked the conformation of compound **5** by 2D NMR. The compound showed similar spectra in DMSO and in water/DMSO mixed solvent, implying an extended conformation (data not shown).

Enzymatic Inhibition Study. The expression and purification of hnp PLA2 were carried out according to accepted methods.^{13,21,29,30} The inhibition studies were carried out using the reported ANS assay.²¹ In the IC_{50} experiment, the concentrations of inhibitors were much higher than that of the enzyme so the binding model was 1:1. Table 1 shows the IC_{50} values of lead compounds **1** and bivalent inhibitors. Compound **2** shows better inhibition ability than **1**, which implies that the linker could increase the binding affinity about 5 times. Also, the bivalent inhibitors are more potent than **2**. Compound **5** is the

best inhibitor with an IC_{50} of 24 nM, approximately 5 times more potent than compound **2**.



To quantitatively calculate the K_{coop} value, another set of enzyme inhibition experiments were performed under special conditions where the concentration of compound **5** was very low: 7.5–40 nM, approximately the same as for the enzyme (30 nM). The binding model was changed to 1:2. Since in the sedimentation experiment, the free enzyme and 1:1 binary complex could not be distinguished, making the K_{coop} value hard to calculate. According to the equations listed in the Experimental Section, the two association constants were calculated to be $K_{a1} = (5.5 \pm 0.3) \times 10^7 \text{ M}^{-1}$, $K_{a2} = (1.1 \pm 0.1) \times 10^8 \text{ M}^{-1}$, and $K_{\text{coop}} = 2.0$.

Discussion

In the current study, we determined the orientation of the two protein molecules by docking them together using the FTDOCK program. We have compared this computational model with the reported crystal structure of porcine pancreatic IB phospholipase A2 dimer and found that the molecular orientation, binding interface, and interaction residues were quite similar. The 19 interface residues in the porcine pancreatic IB phospholipase A2 dimer (nonpolar, L2, W3, L19, M20, L31, V65, and L118; polar, N23, N24, D66, N67, Y69, T70, S72, N117, D119, and T120) were somewhat changed in hnp PLA2 (nonpolar, L2, V3, A18, L19, F23, V30, and F63; polar, H6, E16, E55, K62, Y111, S113, and K115). The nonpolar residues surrounded the opening of active site, showing that the pocket was a hydrophobic capsule. It was possible that the alkyl linker of ligand interacted with these nonpolar residues while the other end of the ligand was free. Herein, ligands that could not drive protein dimerization also showed low IC_{50} values.

We tested the ability of the bivalent ligands to induce dimerization. Bivalent inhibitors with linkers of varying lengths and positions showed different dimer induction abilities. Dimerization ability decreased rapidly when the alkyl chain length was increased from 5 to 7. The ability was also influenced by the parity of chain length. This suggested that the conformation of the dimer and inhibitor was relatively rigid. There is little room in the interior of the capsule for a redundant linker. The *i*-face interacts specifically through electrostatic and hydrophobic interactions, which might be quite weak between free PLA2 molecules, as no dimer could be detected in solution by the analytical ultracentrifugation study. These interactions become significant in the enzyme dimer, with the bivalent molecule contributing to the stability of the ternary complex. Jain³¹ and his co-workers reported that short-range specific binding interactions along the *i*-face and their effect on the hydrogen bonding network provide the basis for the K_{s}^* - and k_{cat}^* allostery. This would help to explain the stability of the ternary complex. Thus,

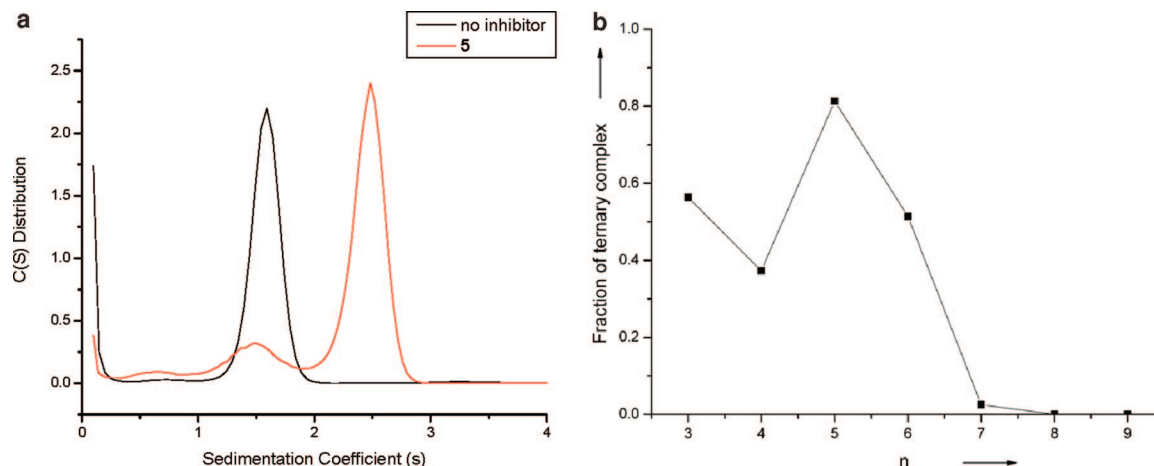


Figure 3. (a) Sedimentation coefficient and distribution $c(s)$ of hnpS PLA2. The black line is the free enzyme, indicating a monomeric form. The red line comes from the mixture of hnpS PLA2 and **5**. The main peak shifted to a larger $c(s)$ corresponding to the dimer. The concentrations of the enzyme and inhibitor **5** were 50 and 25 μM , respectively. Only the complex of **5** was shown here. For other compounds, refer to the figure in Supporting Information. (b) Relationship of the length of alkyl chain (n) and the fraction of ternary complex for compounds **3–9**. **10** and **11** cannot induce dimerization of PLA2 (not shown).

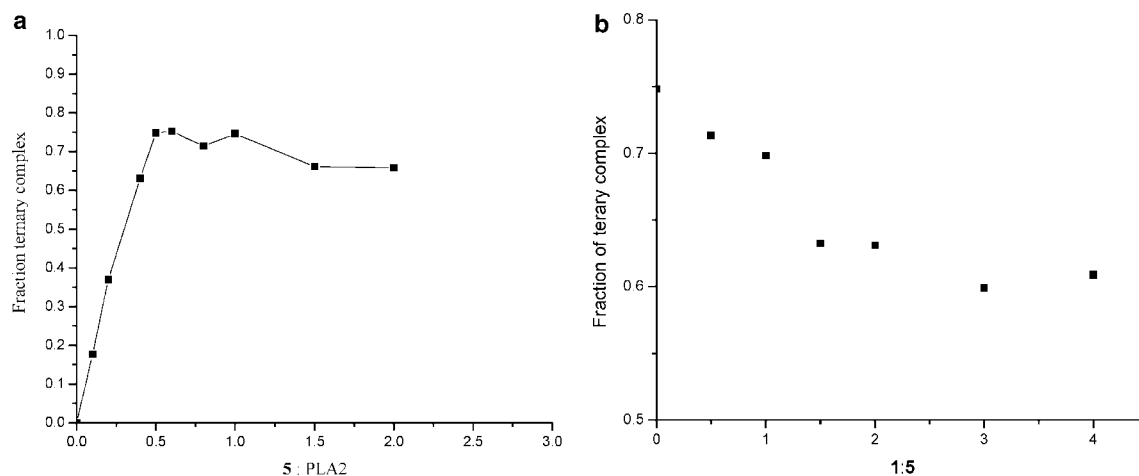


Figure 4. (a) Fraction of protein in the ternary complex is shown as a function of the ratio of dimerizer (**5**) to protein (PLA2). (b) Competitive displacement of **5** by **1**.

Table 1. Enzyme (hnpS PLA2) Inhibition Activities of Bivalent Ligands with Different Chain Lengths and Positions

compd	n	linker position	IC ₅₀ , nM
1			540 ± 110
2	5	<i>o</i>	120 ± 20
3	3	<i>o</i>	48 ± 10
4	4	<i>o</i>	60 ± 10
5	5	<i>o</i>	24 ± 8
6	6	<i>o</i>	39 ± 10
7	7	<i>o</i>	52 ± 4
8	8	<i>o</i>	58 ± 7
9	9	<i>o</i>	49 ± 5
10	5	<i>m</i>	76 ± 20
11	5	<i>p</i>	86 ± 4

the interaction at the *i*-face is complicated but important to dimer formation and enzymatic activity.

To establish a binding model, the two association constants of **5** with the enzyme molecule were calculated. Kopytek, et al. recommended a method to simulate the K_{coop} value of the bivalent inhibitor bisMTX.⁴ In their work, the K_{a1} value for the binding of bisMTX with *E. coli* DHFR was taken approximately as the K_{a} value for the binding of MTX and DHFR. However, the method is not suitable here. For the case of PLA2 inhibitors, the K_{a1} value changed when the linker was added to the

monomer probably because of the hydrophobic nature of the binding pocket (Lu Zhou et al., unpublished results). Therefore, an enzymatic inhibition study was performed to calculate the two association constants of **5**. The enzymatic activities were measured at different **5** concentrations to fit K_{a1} ($5.5 \times 10^7 \text{ M}^{-1}$), K_{a2} ($1.1 \times 10^8 \text{ M}^{-1}$), and K_{coop} ($K_{\text{a2}}/K_{\text{a1}}$). K_{coop} was 2.0, indicating that the protein–protein contacts also contribute to the stability of the ternary complex, as noncooperative binding should give a K_{coop} of 1.

The ability to induce protein dimerization and the difference between the two association constants make compound **5** potentially useful in clinical applications. Because it was reported that a high concentration of hnpS PLA2 was detected in rheumatoid arthritis patients, a compound like **5** could be used to regulate the concentration of effective hnpS PLA2. When the enzyme concentration is high, the compound can form a ternary complex with excess enzyme. When the enzyme concentration is low, as the first order binding constant K_{a1} is not that strong, some of the enzyme molecules may form binary complexes with the compound while the rest remain free to perform their normal physiological functions. Of course, there is still a long way to go before putting this regulatory method into clinical usage.

Here, we have synthesized a series of bivalent compounds, 1, ω -bis(((3-acetamino-5-methoxy-2-methylindole)-2-methylene)phenoxy)alkane, to drive the CID of hnpS PLA2. The ability of these dimeric compounds to drive the assembly of monomeric hnpS PLA2 into the ternary complex was shown *in vitro* by analytical ultracentrifugation analysis. The inhibition strengths of these compounds were tested using a continuous fluorescence assay. The dimerization ability of the inhibitors was found to be related to the linker length and position. Quantitative analysis of the association constants for the strongest binding compound, **5**, revealed that the ternary complex forms mainly by the binding of the bivalent **5** to two enzyme molecules, with some contribution from interactions between the two enzyme molecules. The combination of bis-indole derivatives and hnpS PLA2 can be used as a novel CID system for regulating biological networks.

Experimental Section

Chemistry. Melting points were recorded on an X4 apparatus and are uncorrected. Yields refer to isolated products. ^1H NMR spectra were measured on a Varian Mercury 300 M spectrometer using TMS as internal standard. Mass spectra were recorded on a VG-ZAB-HS spectrometer. Elemental analyses were performed on an Elementar Vario EL instrument. All reactions were monitored by thin layer chromatography, carried out on silica gel 60 F-254 aluminum sheets using UV light (254 and 366 nm). The reagents and solvents were commercially available and purified according to conventional methods.

General Procedure for the Preparation of 1,5-Bis((2-hydroxyethyl)phenoxy)pentane (Compound 15). A solution of 2-hydroxybenzyl alcohol (**12**, 1.86 g, 15mmol) and anhydrous potassium carbonate (2.07 g, 15mmol) in 30 mL of CH_3CN was added into 1, 5-dibromopentane (1.15 g, 5 mmol). Then the solution was heated slowly to reflux and maintained at reflux until **1a** was consumed (TLC monitor, about 6 h). The reaction mixture was cooled and concentrated at reduced pressure, and the residue was separated by column chromatography (silica gel, the eluting solvent ranged from hexane to 50% EtOAc/hexane). An amount of 1.44 g of **15** was obtained, with a yield of 91%. ^1H NMR (CDCl_3) δ 7.22–7.25 (m, 4H), 6.90–6.95 (m, 4H), 4.68 (s, 4H), 4.05 (t, 3H), 2.8 (br s, 1H), 1.85–1.92 (m, 4H), 1.69–1.72 (m, 2H).

13, 14, 16–19 were synthesized following a similar procedure.

General Procedure for the Preparation of 1,5-Bis((2-chloroethyl)phenoxy)pentane (Compound 22). A solution of **15** (1.26 g, 4mmol) and triphenylphosphine (2.62 g, 10mmol) in 20 mL of anhydrous CCl_4 was heated to reflux and maintained at reflux for about 5 h. After the reaction mixture was cooled to room temperature, the mixture was concentrated at reduced pressure and the residue was separated by column chromatography (silica gel, the eluting solvent ranged from hexane to 33% EtOAc/hexane). Pure **22** weighed 0.75 g (yield 53%). ^1H NMR (CDCl_3) δ 7.19–7.33 (m, 4H), 6.86–6.97 (m, 4H), 4.67 (s, 4H), 4.00–4.06 (t, 3H), 1.90–1.96 (m, 4H), 1.75–1.81 (m, 2H).

20, 21, 23–26 were synthesized by a similar procedure.

General Procedure for the Preparation of 1,5-Bis(((3-acetamino-5-methoxy-2-methylindole)-2-methylene)phenoxy)pentane (Compound 5). Under the protection of nitrogen, a solution of 5-methoxy-2-methyl-1*H*-indole-3-acetamide (0.77 g, 3.5mmol) and 50% sodium hydride (0.25 g, 5 mmol) in 10 mL of anhydrous DMF was stirred at room temperature for about 0.5 h. Then **22** (0.57 g, 1.6mmol) was slowly added, and the solution was stirred for 6 h at room temperature. The solution was poured into 70 mL of water and then stirred for about 2 h. The solid was filtered with suction and washed with cold diethyl ether. The product was recrystallized by EtOAc and weighed 0.60 g (yield 52%), mp 168–171 °C. ^1H NMR (CDCl_3): δ 7.19–7.26 (t, 2H) 7.16 (d, 2H, $J = 1.2$), 6.91–7.07 (m, 4H), 6.69–6.74 (m, 4H), 6.23–6.26 (d, 2H), 5.5–5.6 (d, 4H), 5.26 (s, 4H), 4.13 (t, 4H, $J = 4.2$), 3.81 (s, 6H),

3.67 (s, 4H), 2.24 (s, 6H), 2.01–2.04 (m, 4H), 1.78 (m, 2H). MS 717 ($M + 1$). Anal. ($\text{C}_{43}\text{H}_{48}\text{N}_4\text{O}_6$).

3, 4, 6–11 were synthesized by a similar procedure.

1,3-Bis(((3-acetamino-5-methoxy-2-methylindole)-2-methylene)phenoxy)propane (3). The product was recrystallized by EtOAc, and the yield was 66%, mp 123–125 °C. ^1H NMR (CDCl_3) δ 7.19–7.23 (m, 2H), 6.96–7.01 (m, 6H), 6.69–6.74 (m, 6H), 6.25–6.28 (d, 2H), 5.64 (s, 2H), 5.36 (s, 2H), 5.26 (s, 4H), 4.28 (t, 4H, $J = 3.8$), 3.83 (s, 6H), 3.68 (s, 4H), 2.22 (s, 6H), 1.84 (m, 2H). Anal. ($\text{C}_{41}\text{H}_{44}\text{N}_4\text{O}_6$).

1,4-Bis(((3-acetamino-5-methoxy-2-methylindole)-2-methylene)phenoxy)butane (4). The product was recrystallized by EtOAc, and the yield was 24%, mp 138–141 °C. ^1H NMR (CDCl_3): δ 7.19–7.23 (m, 6H), 6.93–6.96 (m, 4H), 6.69–6.74 (m, 2H), 6.24 (d, 2H), 5.64 (s, 2H), 5.32 (s, 2H), 5.22 (s, 4H), 4.65 (t, 4H), 4.20 (s, 6H), 4.10 (s, 4H), 2.42 (s, 6H), 2.09 (m, 4H). Anal. ($\text{C}_{42}\text{H}_{46}\text{N}_4\text{O}_6$).

1,6-Bis(((3-acetamino-5-methoxy-2-methylindole)-2-methylene)phenoxy)hexane (6). The product was recrystallized by EtOAc, and the yield was 29%, mp 196–198 °C. ^1H NMR (CDCl_3): δ 7.06–7.17 (m, 4H), 6.86–6.91 (m, 4H), 6.72–6.77 (m, 4H), 6.23–6.27 (d, 2H), 5.66 (s, 2H), 5.41 (s, 2H), 5.27 (s, 4H), 4.10 (t, 4H, $J = 6.4$), 3.84 (s, 6H), 3.68 (s, 4H), 2.27 (s, 6H), 1.94 (m, 4H), 1.65 (m, 4H). Anal. ($\text{C}_{44}\text{H}_{50}\text{N}_4\text{O}_6$).

1,7-Bis(((3-acetamino-5-methoxy-2-methylindole)-2-methylene)phenoxy)heptane (7). The product was recrystallized by EtOAc, mp 146–149 °C. ^1H NMR (CDCl_3): δ 7.27 (s, 2H), 7.12 (m, 8H), 6.84 (s, 2H), 6.65 (m, 4H), 6.18–6.22 (d, 2H), 5.23 (s, 4H), 4.09 (t, 4H, $J = 7.0$), 3.73 (s, 6H), 3.43 (s, 4H), 2.24 (s, 6H), 1.82 (m, 4H), 1.51 (m, 6H). Anal. ($\text{C}_{45}\text{H}_{52}\text{N}_4\text{O}_6$).

1,8-Bis(((3-acetamino-5-methoxy-2-methylindole)-2-methylene)phenoxy)octane (8). The product was recrystallized by EtOAc, mp 108–110 °C. ^1H NMR (CDCl_3): δ 7.27 (s, 2H), 7.12 (m, 8H), 6.84 (s, 2H), 6.64–6.70 (m, 4H), 6.18–6.21 (d, 2H), 5.23 (s, 4H), 4.06 (t, 4H, $J = 5.6$), 3.73 (s, 6H), 3.43 (s, 4H), 2.24 (s, 6H), 1.81 (m, 4H), 1.45 (m, 8H). Anal. ($\text{C}_{46}\text{H}_{54}\text{N}_4\text{O}_6$).

1,9-Bis(((3-acetamino-5-methoxy-2-methylindole)-2-methylene)phenoxy)nonane (9). The product was recrystallized by EtOAc, mp 112–115 °C. ^1H NMR (CDCl_3): δ 7.27 (s, 2H), 7.12 (m, 6H), 6.97–7.01 (m, 2H), 6.85 (s, 2H), 6.65–6.71 (m, 4H), 6.18–6.21 (d, 2H), 5.24 (s, 4H), 4.05 (t, 4H, $J = 4.6$), 3.73 (s, 6H), 3.43 (s, 4H), 2.25 (s, 6H), 1.79 (m, 4H), 1.39 (m, 10H). Anal. ($\text{C}_{47}\text{H}_{56}\text{N}_4\text{O}_6$).

1,5-Bis(((3-acetamino-5-methoxy-2-methylindole)-3-methylene)phenoxy)pentane (10). The product was recrystallized by EtOAc, and the yield was 88%, mp 110–112 °C. ^1H NMR (CDCl_3): δ 7.12–7.17 (m, 4H), 6.96–6.97 (m, 2H), 6.73–6.82 (m, 4H), 6.49–6.53 (m, 4H), 5.66 (s, 2H), 5.54 (s, 2H), 5.24 (s, 4H), 3.86 (m, 10H), 3.68 (s, 4H), 2.31 (s, 6H), 1.73–1.78 (m, 4H), 1.54–1.56 (m, 2H). Anal. ($\text{C}_{43}\text{H}_{48}\text{N}_4\text{O}_6$).

1,5-Bis(((3-acetamino-5-methoxy-2-methylindole)-4-methylene)phenoxy)pentane (11). The product was recrystallized by EtOAc, and the yield was 32%, mp 160–165 °C. ^1H NMR (CDCl_3): δ 7.12–7.17 (d, 2H) 6.97 (d, 2H, $J = 2.2$), 6.90 (m, 4H), 6.78–6.83 (m, 6H), 5.41 (s, 2H), 5.62 (s, 2H), 5.21 (s, 4H), 3.90 (t, 4H), 3.84 (s, 6H), 3.67 (s, 4H), 2.30 (s, 6H), 1.80 (m, 4H), 1.65 (m, 2H). Anal. ($\text{C}_{43}\text{H}_{48}\text{N}_4\text{O}_6$).

5-Methoxy-2-methyl-1*H*-1-(*o*-pentoxy)benzylindole-3-acetamide (2). The product was recrystallized by ether, and the yield was 75%, mp 136–138 °C. ^1H NMR (CDCl_3): δ 7.16 (m, 3H), 6.85 (m, 2H), 6.66–6.72 (m, 2H), 6.23 (d, 1H), 5.25 (s, 2H), 4.07 (m, 2H), 3.75 (s, 3H), 3.44 (s, 3H), 2.25 (s, 3H), 1.82 (m, 2H), 1.36–1.50 (m, 6H), 0.92 (t, 3H). Anal. ($\text{C}_{24}\text{H}_{30}\text{N}_2\text{O}_3$).

Analytical Ultracentrifugation Analysis. Sedimentation velocity experiments were conducted on a Beckman Optima XLA analytical ultracentrifuge equipped with absorbance optics. Data were analyzed with the software Sedfit, version 8.9g. Different inhibitors were tested to examine their ability to induce enzyme dimerization. The concentrations of enzyme and inhibitors were 50 and 25 μM , respectively. The buffer contained 100 mM NaCl, 50 mM Tris-HCl (pH 8.0), and 2% DMSO (v/v).

5 was tested in detail to obtain the data of concentration-dependent and competitive displacement (Figure 4). In the con-

centration-dependent experiment, the concentration of enzyme was 50 μM and that of **5** was changed from 6.25 to 100 μM . In the competitive displacement experiment, the concentrations of enzyme and **5** were 50 and 25 μM and the concentration of competitor was changed from 12.5 to 100 μM .

Enzymatic Inhibition Assay. The assay was carried out in a 96-well plate utilizing a multiwell fluorometer (SpectraMax GeminiXS, Molecular Devices). The hnpS PLA2 was expressed as reported previously.^{13,21,29,30} In brief, a synthesized gene was ligated to a pET21a vector and transformed into *Escherichia coli* cells (BL21(DE3) strain). And there was a refolding process in the purification.²¹ All solutions were prepared with high purity (18 MX conductivity) water. The buffer used in all the experiments was 50 mM Tris, 100 mM NaCl, pH 8.0, 10 μM ANS, 10 mM CaCl_2 . The substrate was 2 mM dimyristoylphosphatidylcholine (DMPC)–deoxycholic acid (DCA) buffer solution, which was sonicated for 1 min to get the micelle suspension. All the samples were dissolved in DMSO. A 200 μL reaction solution contained 15 nM PLA2, 20 μL of substrate, 0.1 mg/mL BSA, and 10 μL of inhibitor solution. The reaction was monitored by excitation at 377 nm and emission at 470 nm. Fluorescent signals were monitored by a kinetics mode program. Reported IC_{50} values, determined by plotting concentration–velocity curves, are the mean of at least three separate experiments. The initial velocities of the change in fluorescence intensity with various inhibitor concentrations were used to calculate the IC_{50} values.

Calculation of K_{coop} Value. For the testing of inhibition activities, the concentration of the inhibitor was much higher than that of the enzyme (50–1000 nM vs 15 nM). Therefore, the interaction of the inhibitor and the enzyme should follow the 1:1 model. However, if the concentrations of the bivalent ligand and the enzyme were comparable (7.5–40 nM vs 30 nM), they may follow the 1:2 binding model; that is, both binary and ternary complexes can form under assay conditions. The equations below describe the possible interactions:



$$[\text{I}]_t = [\text{I}] + [\text{EI}] + [\text{E}_2\text{I}]$$

$$[\text{E}]_t = [\text{E}] + [\text{EI}] + 2[\text{E}_2\text{I}]$$

$$[\text{EI}] = K_{a1}[\text{E}][\text{I}]$$

$$[\text{E}_2\text{I}] = K_{a2}[\text{EI}][\text{E}]$$

where $[\text{I}]_t$ is the total concentration of bivalent ligands, $[\text{I}]$ is the concentration of free bivalent ligands in the solution, $[\text{E}]_t$ is the total concentration of enzyme, $[\text{E}]$ is the concentration of free enzyme in the solution, $[\text{EI}]$ is the concentration of the binary complex of bivalent ligands and the enzyme, and $[\text{E}_2\text{I}]$ is the concentration of the tertiary complex of bivalent ligands and two enzyme molecules.

Here, the interaction between the substrate and PLA2 was neglected because the $[\text{S}]/K_m$ was less than 1 ($K_m = 330 \mu\text{M}$ and $[\text{S}] = 100 \mu\text{M}$). After some mathematic conversion, we get the equation below, which could be used to calculate the two association constants K_{a1} and K_{a2} . And $K_{\text{coop}} = K_{a2}/K_{a1}$.

$$\frac{[\text{I}]_t + [\text{E}] - [\text{E}]_t}{[\text{E}]_t - [\text{E}]}[\text{E}] = -K_{a2} \frac{2[\text{I}]_t + [\text{E}] - [\text{E}]_t}{[\text{E}]_t - [\text{E}]}[\text{E}]^2 + \frac{1}{K_{a1}}$$

Here,

$$A = \frac{2[\text{I}]_t + [\text{E}] - [\text{E}]_t}{[\text{E}]_t - [\text{E}]}[\text{E}]^2$$

and

$$B = \frac{[\text{I}]_t + [\text{E}] - [\text{E}]_t}{[\text{E}]_t - [\text{E}]}[\text{E}]$$

While $[\text{E}]_t$ was a constant (30 nM) and $[\text{I}]_t$ changed from 40 to 7.5 nM, $[\text{E}]$ was calculated according to the experimental result.

Because the velocity of the enzyme hydrolysis reaction and substrate could be described as $v = k[\text{E}][\text{S}]$ and $[\text{S}]$ is almost constant during the experiment, the reaction can be regarded as pseudo-first-order. Thus, $v/v_0 = [\text{E}]/[\text{E}]_t$, where v is the velocity of the reaction with **5** and v_0 is the velocity of the reaction without **5**. According to the equation

$$B = -K_{a2}A + \frac{1}{K_{a1}}$$

we can calculate that $K_{a1} = (5.5 \pm 0.3) \times 10^7 \text{ M}^{-1}$, $K_{a2} = (1.1 \pm 0.1) \times 10^8 \text{ M}^{-1}$, and $K_{\text{coop}} = 2.0$.

Acknowledgment. This project was supported in part by the Ministry of Science and Technology of China, the National Natural Science Foundation of China (Grants 30490245, 90403001, 20473001, 20773002), and China Postdoctoral Science Foundation (Grant 20070410433).

Supporting Information Available: Elemental analysis and analytical ultracentrifugation analysis data for Figure 3 and gel electrophoresis of hnpS-PLA2 purification. This material is available free of charge via the Internet at <http://pubs.acs.org>.

References

- (1) Ullrich, A.; Schlessinger, J. Signal transduction by receptors with tyrosine kinase-activity. *Cell* **1990**, *61*, 203–212.
- (2) Spencer, D. M.; Wandless, T. J.; Schreiber, S. L.; Crabtree, G. R. Controlling signal-transduction with synthetic ligands. *Science* **1993**, *262*, 1019–1024.
- (3) Ho, S. N.; Biggar, S. R.; Spencer, D. M.; Schreiber, S. L.; Crabtree, G. R. Dimeric ligands define a role for transcriptional activation domains in reinitiation. *Nature* **1996**, *382*, 822–826.
- (4) Belshaw, P. J.; Ho, S. N.; Crabtree, G. R.; Schreiber, S. L. Controlling protein association and subcellular localization with a synthetic ligand that induces heterodimerization of proteins. *Proc. Natl. Acad. Sci. U.S.A.* **1996**, *93*, 4604–4607.
- (5) Rivera, V. M.; Clackson, T.; Natesan, S.; Pollock, R.; Amara, J. F.; Keenan, T.; Magari, S. R.; Phillips, T.; Courage, N. L.; Cerasoli, F.; Holt, D. A.; Gilman, M. A humanized system for pharmacologic control of gene expression. *Nat. Med.* **1996**, *2*, 1028–1032.
- (6) Farrar, M. A.; Alberol, I.; Perlmutter, R. M. Activation of the Raf-1 kinase cascade by coumermycin-induced dimerization. *Nature* **1996**, *383*, 178–181.
- (7) Kopytek, S. J.; Standaert, R. F.; Dyer, J. C. D.; Hu, J. C. Chemically induced dimerization of dihydrofolate reductase by a homobifunctional dimer of methotrexate. *Chem. Biol.* **2000**, *7*, 313–321.
- (8) Harvey, I.; Garneau, P.; Pelletier, J. Forced engagement of a RNA/protein complex by a chemical inducer of dimerization to modulate gene expression. *Proc. Natl. Acad. Sci. U.S.A.* **2002**, *99*, 1882–1887.
- (9) Liu, J. Y.; Zhang, Z. S.; Tan, X. J.; Hol, W. G. J.; Verlinde, C. L. M. J.; Fan, E. K. Protein heterodimerization through ligand-bridged multivalent pre-organization: enhancing ligand binding toward both protein targets. *J. Am. Chem. Soc.* **2005**, *127*, 2044–2045.
- (10) Tachedjian, G.; Orlova, M.; Sarafianos, S. G.; Arnold, E.; Goff, S. P. Nonnucleoside reverse transcriptase inhibitors are chemical enhancers of dimerization of the HIV type 1 reverse transcriptase. *Proc. Natl. Acad. Sci. U.S.A.* **2001**, *98*, 7188–7193.
- (11) Berg, T. Modulation of protein–protein interactions with small organic molecules. *Angew. Chem., Int. Ed.* **2003**, *42*, 2462–2481.
- (12) Nevalainen, T. Serum phospholipases A2 in inflammatory diseases. *J. Clin. Chem.* **1993**, *39*, 2453–2457.
- (13) Pruzanski, W.; Vadas, P.; Browning, J. Secretory non-pancreatic group II phospholipase A2: role in physiologic and inflammatory processes. *J. Lipid Mediators* **1993**, *8*, 161–167.
- (14) Gelb, M. H.; Min, J. H.; Jain, M. K. Do membrane-bound enzymes access their substrates from the membrane or aqueous phase: interfacial versus non-interfacial enzymes. *Biochim. Biophys. Acta* **2000**, *1488*, 20–27.
- (15) Berg, O. G.; Yu, B. Z.; Rogers, J.; Jain, M. K. Interfacial catalysis by phospholipase-A2. Determination of the interfacial kinetic rate constants. *Biochemistry* **1991**, *30*, 7283–7297.
- (16) Brunie, S.; Bolin, J.; Gewirth, D.; Sigler, P. B. The refined crystal structure of dimeric phospholipase A2 at 2.5 Å. Access to a shielded catalytic center. *J. Biol. Chem.* **1985**, *260*, 9742–9749.
- (17) Suzuki, A.; Matsueda, E.; Yamane, T.; Ashida, T.; Kihara, H.; Ohno, M. Crystal-structure analysis of phospholipase a(2) from trimeresurus-

- flavoviridis (Habu Snake) venom at 1.5 angstrom resolution. *J. Biochem.* **1995**, *117*, 730–740.
- (18) Pan, Y. H.; Epstein, T. M.; Jain, M. K.; Bahnson, B. J. Five coplanar anion binding sites on one face of phospholipase A(2). Relationship to interface binding. *Biochemistry* **2001**, *40*, 609–617.
- (19) Schevitz, R. W.; Bach, N. J.; Carlson, D. G.; Chirgadze, N. Y.; Clawson, D. K.; Dillard, R. D.; Draheim, S. E.; Hartley, L. W.; Jones, N. D.; Mihelich, E. D.; Olkowski, J. L.; Snyder, D. W.; Sommers, C.; Wery, J. P. Structure-based design of the first potent and selective inhibitor of human nonpancreatic secretory phospholipase-a(2). *Nat. Struct. Biol.* **1995**, *2*, 458–465.
- (20) Dillard, R. D.; Bach, N. J.; Draheim, S. E.; Berry, D. R.; Carlson, D. G.; Chirgadze, N. Y.; Clawson, D. K.; Hartley, L. W.; Johnson, L. M.; Jones, N. D.; McKinney, E. R.; Mihelich, E. D.; Olkowski, J. L.; Schevitz, R. W.; Smith, A. C.; Snyder, D. W.; Sommers, C. D.; Wery, J. P. Indole inhibitors of human nonpancreatic secretory phospholipase A2. 2. Indole-3-acetamides with additional functionality. *J. Med. Chem.* **1996**, *39*, 5137–5158.
- (21) Huang, C. K.; Zhou, L.; Liu, Y.; Lai, L. H. A continuous fluorescence assay for phospholipase A2 with nontagged lipid. *Anal. Biochem.* **2006**, *351*, 11–17.
- (22) Jackson, R. M.; Gabb, H. A.; Sternberg, M. J. E. Rapid refinement of protein interfaces incorporating solvation: application to the docking problem. *J. Mol. Biol.* **1998**, *276*, 265–285.
- (23) Warren, S. C.; DeLano, L. *The PyMOL Molecular Graphics System*; DeLano Scientific LLC: Palo Alto, CA; <http://pymol.sourceforge.net/>.
- (24) Liu, Y.; Han, X. F.; Huang, C. K.; Hao, X.; Lai, L. H. Indole-5-phenylcarbamate derivatives as human non-pancreatic secretory phospholipase A2 inhibitor. *Bioorg. Med. Chem. Lett.* **2005**, *15*, 4540–4542.
- (25) Lebowitz, J.; Lewis, M. S.; Schuck, P. Modern analytical ultracentrifugation in protein science: a tutorial review. *Protein Sci.* **2002**, *11*, 2067–2079.
- (26) Laue, T. M.; Stafford, W. F. Modern applications of analytical ultracentrifugation. *Annu. Rev. Biophys. Biomol. Struct.* **1999**, *28*, 75–100.
- (27) Schuck, P. On the analysis of protein self-association by sedimentation velocity analytical ultracentrifugation. *Anal. Biochem.* **2003**, *320*, 104–124.
- (28) Carlson, J. C. T.; Kanter, A.; Thuduppathy, G. R.; Cody, V.; Pineda, P. E.; McIvor, R. S.; Wagner, C. R. Designing protein dimerizers: the importance of ligand conformational equilibria. *J. Am. Chem. Soc.* **2003**, *125*, 1501–1507.
- (29) Othman, R.; Baker, S.; Li, Y.; Worrall, A. F.; Wilton, D. C. Human non-pancreatic (group II) secreted phospholipase A(2) expressed from a synthetic gene in *Escherichia coli*: characterisation of N-terminal mutants. *Biochim. Biophys. Acta* **1996**, *2*, 92–102.
- (30) Han, S. K.; Lee, B. I.; Cho, W. H. Bacterial expression and characterization of human pancreatic phospholipase A(2). *Biochim. Biophys. Acta* **1997**, *1346*, 185–192.
- (31) Jain, M. K.; Berg, O. G. Coupling of the i-face and the active site of phospholipase A(2) for interfacial activation. *Curr. Opin. Chem. Biol.* **2006**, *10*, 473–479.

JM7010707